

REDSIM Task B. Report on mapping crop attributes and surface fluxes

Authors: S.G. García Galiano, A. Baille, R. García Cárdenas.

Introduction

The potential of remote sensing for the recommendation and monitoring of irrigation practices, is irrefutable. The context of uncertainty in the rural areas of the southwest Mediterranean area, especially in agriculture, is caused by the loss of competitiveness and abandonment of farming in many areas due to problems related to water scarcity and increase of drought events.

The Southeastern Spanish basins, are regularly affected by drought. These events affect large areas, and its severity has increased in recent years due to climate change (García Galiano *et al.*, 2011). This situation endangers the continuity of significant areas of irrigation, critical in this case for the economy of the Region of Murcia. Moreover, the adjusted water allocations for irrigation in the Region, coupled with quality problems that necessarily arise from the intensive use of resources will continue setting up a situation of scarcity, it is conceivable that repeated acute episodes of lack of water for irrigation, such as those registered in recent years and there will have to face in the coming decades with greater intensity.

As a result, the assessment and monitoring of irrigated areas presents special relevance. Remote sensing has proved to be a very efficient tool for this, allowing the estimation of vegetation indices related to the soil water content, and actual evapotranspiration directly. The present study addresses the operational development below an GIS (Geographical Information System) environment, a remote sensing based methodology for estimating crop attributes and surface fluxes (actual evapotranspiration) and its application in the Region of Murcia.

The potential of remote sensing in agriculture is high, because multispectral reflectance and temperatures of the crop canopies are related to photosynthesis and evapotranspiration (Basso *et al.*, 2004). Several studies present methodologies for the assessment of water stress indices from remote sensing (Moran *et al.*, 1994; Fensholt and Sandholt, 2003). The classical method for the monitoring and evaluation of vegetation water stress is the combined use of land surface temperature (LST) data and multispectral reflectance of the surface, from which the normalized difference vegetation index (NDVI) is derived. The information on wavelengths of the thermal region and visible / near-infrared (NIR), is relevant and useful for the purpose of monitoring the physiological state of vegetation and its level of stress, and especially the intensity of water stress.

In the assessment of the onset, severity, and duration of water stress and drought situations, indicators can be based on meteorological and crop data, or be indicators based only on remote sensing, or be process-based indicators.

Regarding the *indicators based on meteorological data*, the Crop Water Stress Index (CWSI) proposed by (Moran *et al.*, 1994), is widely applied. But the CWSI index, useful for surfaces completely covered with vegetation, requires a great deal of information in order to be applied.

As for *indicators based on remote sensing*, different methodologies of operational assessment of indices related with water deficit of soil and vegetation stress, soil moisture or directly from remote sensing could be applied. However, remote sensing-based products must be calibrated with ground data (ground truth). There will be a literature review of the main sensors currently used in relation to soil moisture estimation from remote sensing.

Soil moisture estimates can be obtained from various satellites, such as ERS SAR (European Remote Sensing Satellites, Synthetic Aperture Radar), Radarsat, ENVISAT ASAR, ADEOS II and EOS PM sensor AMSR (Advanced Microwave Scanning Radiometer). But most of them do not have temporal resolutions appropriate for monitoring highly dynamic processes. Among the latest tools that are available, the MIRAS (Microwave Imaging Radiometer using Aperture Synthesis) sensor of SMOS (Soil Moisture and Ocean Salinity) mission of the European Space Agency (ESA, 2009) should be highlighted. In all cases, the indicators (or variables) derived from remote sensing data must be validated in situ (ground truth).

In the case of *indicators estimated from remote sensing*, there indices that include ratios of two or more bands in the visible and NIR wavelengths (such as NDVI, etc.), and those obtained from the interpretation of LST-NDVI trapezoid (*Vegetation Index/Temperature Trapezoid*). These last include the Water Deficit Index (WDI) proposed by Moran *et al.* (1994) considering the Soil Adjusted Vegetation Index (SAVI) (Huete, 1988). The WDI index has been used to estimate evapotranspiration rates for mixed surfaces, while the CWSI index is specific for areas completely covered by vegetation. The WDI index reaches a value of 1 for conditions of extreme stress of the vegetation, and 0 for crop evaporation to its potential rate. The WDI index has been reformulated by Verstraeten *et al.* (2001), considering only terms of LST and air temperature.

Then Wang (2001) proposed the Vegetation Temperature Condition Index (VTCI), in which the surface temperature-NDVI space behaved like a triangle. This methodology has been widely used in the U.S. Southern Plains (Wan *et al.*, 2004).

The Temperature-Vegetation Dryness Index (TVDI), proposed by Sandholt *et al.* (2002), is obtained from space LST-NDVI and can be used as an indicator of soil moisture and hence the vegetation water stress. Particularly in the rainy season, indices related to soil moisture obtained from wavelengths in the infrared short-wave and NIR can be a valuable supplement to the method based on LST-NDVI space interpretation. Since LST is very sensitive to atmospheric effects and clouds, the use of the SIWSI (Shortwave Infrared Water Stress Index) index, using near-infrared data (Fensholt and Sandholt, 2003) has been considered. According to these authors, working in areas of West Africa, the SIWSI is strongly related to soil moisture, and can be obtained even in the presence of clouds. Although from previous studies in the southeast Spanish (Garcia *et al.*, 2006) it is not an appropriate index in semi-arid watersheds.

The STI Index (Standardized Thermal Index), obtained from data of air temperature and LST, may also constitute a relevant indicator of relative deficit of soil moisture (Park *et al.*, 2004).

Finally, *indicators based on processes* are regarding with the modeling of actual evapotranspiration (ET_{act}). The methods considered simulate the mass and energy transfer between the atmosphere and surface.

Indices based on ratios of two or more bands in the visible and NIR wavelengths

- NDVI (Normalized Difference Vegetation Index)

The Normalized Difference Vegetation Index (NDVI, Kriegler, 1969; Rouse *et al.*, 1973), is based on the assumption that the vegetation subject to water stress presents a greater reflectivity in the visible region (0.4-0.7 μ) of the electromagnetic spectrum and a lower reflectance in the NIR region (0.7-1.1 μ). The NDVI is obtained by the following equation, where NIR is the near-infrared reflectivity and R corresponds to the red region of the electromagnetic spectrum.

$$NDVI = \frac{NIR - R}{NIR + R} \quad (1)$$

This index could be easily derived with the satellite information, using bands 1 and 2 in the case of AVHRR sensor (NOAA), or bands 3 and 4 in the case of ETM+ (Landsat). NDVI vary between -1 and 1.

- **RVI (Ratio Vegetation Index)**

This RVI (Ratio Vegetation Index, Jordan, 1969), is estimated as,

$$RVI = \frac{NIR}{R} \quad (2)$$

- **GNDVI (Green Normalized Difference Vegetative Index) and DVI (Difference Vegetation Index)**

The GNDVI (Green Normalized Difference Vegetative Index) is a modification of NDVI where the Red band is substituted by the reflectance in the Green band (Gitelson *et al.*, 1996).

In the case of DVI (Difference Vegetation Index, Richardson and Everitt, 1992), is estimated as follows,

$$DVI = NIR - R \quad (3)$$

- **SAVI (Soil Adjusted Vegetation Index)**

The SAVI (Soil Adjusted Vegetation Index) proposed by Huete (1988), takes into account the optical soil properties on the plant canopy reflectance. SAVI is involving a constant L to the NDVI equation, and with a range -1 to +1, is expressed as follows,

$$SAVI = \frac{NIR - R}{NIR + R + L} (1 + L) \quad (4)$$

Two or three optimal adjustment for L constant ($L=1$ for low vegetation; $L=0.5$ for intermediate vegetation densities; $L= 0.35$ for higher densities), are suggested by Huete (1988).

- **TSAVI (Transformed Adjusted Vegetation Index)**

The TSAVI (Transformed Adjusted Vegetation Index) original method was modified by Baret and Guyot (1991), as follows,

$$TSAVI = a \frac{NIR - aR - b}{aNIR + R - ab + \chi(1 + a^2)} \quad (5)$$

where a and b are soil line parameters, and X is 0.08. TSAVI varies from 0 for bare soil to 0.7 for very dense canopies (Baret and Guyot, 1991).

Interpretation of LST - NDVI space

The combination of LST and NDVI can provide information about the condition of vegetation and moisture on the surface. The combined information on the wavelengths of the thermal region and the visible/NIR region has proved satisfactory for monitoring vegetation conditions and stress, especially water stress. Numerous studies have provided different interpretations of space LST-NDVI, based on a wide range of vegetation types and crops, climate, and different scales.

The NDVI is a rather conservative indicator of water stress, because the vegetation remains green after the start of this stress. By contrast, the LST increases rapidly with the water stress (Sandholt *et al.*, 2002). For a given dry zone, the relationship between LST and the NDVI is characterized by a cloud of dispersion in the LST-NDVI space, the highest values of LST correspond to the lowest values of NDVI (Nemani and Running, 1989). This relationship is often expressed by the slope of a line fitted to the dry edge of the space LST-NDVI.

Numerous studies have focused on the relationship between LST and the NDVI, to provide indirect information about the vegetation stress and the soil moisture conditions. Nemani and Running (1989) related the slope LST-NDVI to stomatal resistance and evapotranspiration of a deciduous forest. Boegh *et al.* (1998) and Jiang and Islam (1999), related the slope LST-NDVI to surface evapotranspiration. The analysis of LST-NDVI space was also used to derive information on conditions of regional soil moisture (Carlson and Gillies, 1993; Goetz, 1997, Goward *et al.*, 2002 and Sandholt *et al.*, 2002).

Often the estimate of the slope LST-NDVI is not direct (Troufleau and Soegaard, 1998), typically due to the significant variability caused by surface heterogeneity (Czajkowski, 2000). The scattering cloud formed by the LST and NDVI (or vegetation index) both derived from remote sensing, often results in a triangular (Price, 1990, Carlson *et al.*, 1994) or trapezoidal (Moran *et al.*, 1994) shape, if the data represent a full range of vegetation covers and soil moisture content. Different types of surfaces can have different slopes LST-NDVI and intercept the atmospheric conditions and surface moisture equally; the choice of scale can influence the shape of the relationship between these variables (Sandholt *et al.*, 2002).

The vegetation index is linearly related to vegetation cover, and the gradient LST-air temperature is as a function of vegetation index. Assuming these premises, Moran *et al.* (1994) derived the shape of LST-NDVI space from modeling and proposed a theoretical justification for the concept.

The interpretation of the LST for bare soil is not straightforward, because the measured temperature integrates both the temperature of the soil surface temperature and vegetation temperature, and the components cannot be linearly related. Other studies have shown that, at least for well irrigated areas, the relationship between LST and the NDVI is more directly related to the moisture of the soil surface (Friedl and Davis, 1994).

Moran *et al.* (1994) combined the method of LST-NDVI space with standard meteorological data, as well as remote sensing data, to estimate the Water Deficit Index (WDI). They used the temperature difference between LST and air temperature ($\Delta T_s = LST - T_a$) and its relationship to vegetation index. This method was studied for partially vegetated surfaces, and the cloud of dispersion of the values LST-NDVI presented a trapezoidal shape.

Sandholt *et al.* (2002) presented a simplification of the WDI index, which considers the variations in air temperature, water balance and atmospheric conditions to estimate the LST-NDVI space. The method is conceptually and computationally straightforward, and only uses information from satellites to define the Temperature-Vegetation Dryness Index (TVDI), which is related to soil moisture.

Other authors, such as Prihodko and Goward (1997), proposed the Temperature-Vegetation Index (TVX), estimated as a slope in the LST-NDVI space for a homogeneous area with little or no variation in surface moisture conditions. This method, like that proposed by Sandholt *et al.* (2002), does not requires auxiliary data. This is an advantage over other methods for defining the limits of LST-NDVI space, with high requirements of detailed information about weather conditions, including vapor pressure deficit, wind speed and surface resistance.

Adapting the method proposed by Sandholt *et al.* (2002), described above, the location of a pixel in the LST-NDVI space is determined by several factors:

- Vegetation cover

The vegetation cover does not necessarily have to be related to spectral vegetation indices through a simple linear transformation. Furthermore, the fraction of vegetation cover affects the amount of bare soil and

vegetation, visible by the sensor. Thus the LST can be affected by differences in temperature radiated by the bare soil and by sparse vegetation

- Evapotranspiration (ET)

The evapotranspiration can control the LST by the surface energy balance. To lower evapotranspiration, more energy will be available for heating the surface. The stomatal resistance, which characterizes the control of the plants to water vapor transfer by transpiration, is a key parameter in the estimation of ET. With greater stress of plants, there is therefore more resistance of the plants to water transfer. This resistance can be expressed in terms of soil factors (soil moisture or soil water potential) and of climate factors (radiation, relative humidity and air temperature).

- Thermal properties of the surface

In the case of partially vegetated surfaces, LST is influenced by the heat capacity and thermal conductivity of the soil. These properties are a function of soil type, and change with the soil moisture.

- Net radiation

The available energy, incident on the surface, affects the LST. The radiation control of LST implies that areas with high albedo values present low temperatures. The albedo is controlled by the type of soil, surface soil moisture and vegetation cover.

- Weather conditions and surface roughness

The ability to transfer energy from the surface to the atmosphere is an important factor in controlling the LST. The concept of *surface resistance* is used to quantify this ability to transfer sensible and latent heat (evaporation).

This resistance depends on the surface roughness, wind speed and atmospheric stability conditions. Under similar conditions of leaf area index and water availability, the vegetation cover with high roughness (forests) and low surface resistance will have lower LST than surfaces with low roughness (low vegetation) and higher surface resistance. This influences the shape of LST-NDVI space.

The above-mentioned factors have been summarized in Fig. 1. It is clear that the relationship between LST and surface soil moisture is not straightforward. For bare soil with constant irradiance, the LST is defined primarily by the soil moisture content, via control of evaporation and thermal properties of the surface (Sandholt *et al.*, 2002).

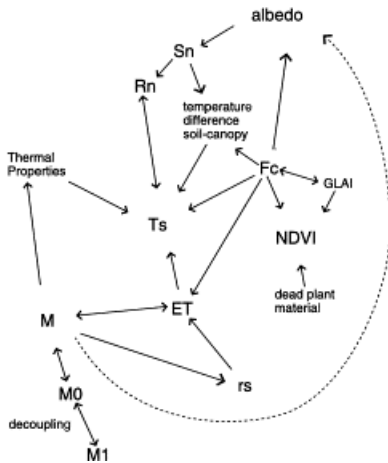


Fig. 1. Factors for the definition of LST of the illuminated surface (adapted from Sandholt *et al.*, 2002).

From Fig. 1 above, variables enclosed by the circle can be estimated using satellite data. S_n = shortwave net radiation; R_n = net radiation; $GLAI$ = leaf area index; F_c = fraction of soil covered by vegetation; ET = evapotranspiration; rs = stomatal resistance; $M1$ = soil moisture content (root zone); $M0$ = moisture content of top soil.

In Fig. 2 depicts the concept of LST-NDVI space. The left edge represents bare soil from dry to wet (top-down) range. As the amount of green vegetation increases, the NDVI value also increases along the X axis and therefore the maximum LST decreases. For dry conditions, the negative relationship between LST and NDVI is defined by the upper edge, which is the upper limit of LST for a given type of surface and climatic conditions (Sandholt *et al.*, 2002).

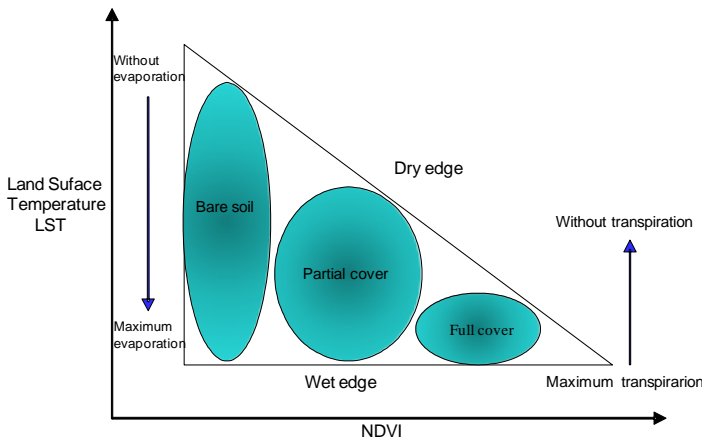


Fig. 2. Simplified LST/NDVI space (adapted from Lambin and Ehrlich, 1996 in Sandholt *et al.*, 2002).

• TVDI index

For deriving information regarding with content of surface soil moisture, Sandholt *et al.* (2002) proposed an index of aridity (TVDI), that takes values of 1 for the dry edge (limited water availability) and 0 for the wet edge (maximum evapotranspiration and thereby unlimited water availability).

The TVDI is related to soil moisture, where high values indicate dry conditions and low values wet conditions. This is based on the fact that the LST is mainly controlled by the energy balance and thermal inertia, factors influencing moisture conditions at the surface and in the root zone (Andersen *et al.*, 2002).

Following the concept in Fig. 3, the value of TVDI for a given pixel in the LST-NDVI space, is calculated as the ratio of lines A and B, and therefore calculated using the following equation (Sandholt *et al.* 2002),

$$TVDI = \frac{A}{B} = \frac{LST - LST_{\min}}{a + bNDVI - LST_{\min}} \quad (6)$$

where LST_{\min} is the minimum LST in the triangle, defining the wet edge, and LST corresponds to the pixel. Then, a and b are the coefficients of the regression line that define the dry edge, as follows,

$$LST_{\max} = a + bNDVI \quad (7)$$

where LST_{\max} is the maximum LST for a certain NDVI.

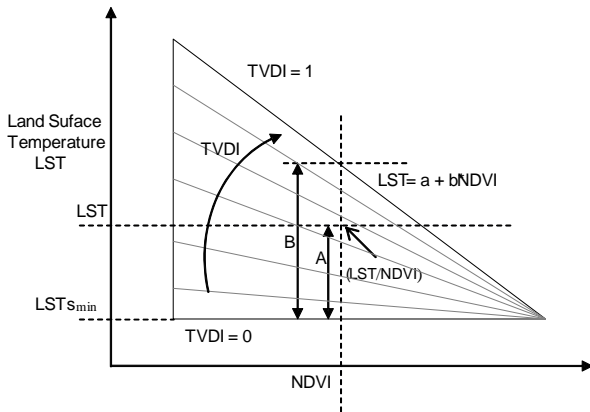


Fig. 3. Definition of TVDI index (adapted from Sandholt *et al.*, 2002).

The parameters a and b are estimated based on pixels from an large enough area to represent the full range of surface soil moisture content, from wet to dry, and from bare soil to fully vegetated surfaces.

Uncertainty about TVDI is greater in the high range of NDVI, where the TVDI isolines are grouped. The simplification of representing LST-NDVI with a triangle instead of a trapezoid (eg Moran *et al.*, 1994) may add uncertainty to TVDI estimation for high values of NDVI. The wet edge is also modeled as a horizontal line as opposed to an inclined one, as in the trapezoidal method, which can lead to an overestimation of TVDI for low NDVI.

The TVDI isolines correspond to the TVX index, proposed by Prihodko and Goward (1997), thus being able to estimate such TVDI isolines as multiple superimposed TVX lines. For drier conditions, several studies of LST-NDVI spaces present steep slopes (eg, Goetz, 1997 and Nemani *et al.*, 1993), which is consistent with TVDI. Since TVDI can be estimated for each pixel, the spatial resolution of the data is fully maintained. TVX requires an area wide enough for determination of the slope in the LST-NDVI space.

The main advantages of TVDI are: (i) its simplicity of calculation; and (ii) its derivation from satellite data alone regardless of factors such as weather, vapor pressure deficit, wind speed and surface resistance. However, this approach requires a large number of remote sensing observations to accurately define the limits of that space (Sandholt *et al.*, 2002).

• Water Deficit index

The Water Deficit Index (WDI, Moran *et al.* 1994), to estimate evapotranspiration in both areas completely covered by vegetation or partially covered, is based on the interpretation of the trapezoid formed by the relationship between the difference in LST and air temperature versus vegetation cover fraction (or vegetation index). The WDI quantifies the relative rate of latent heat flux, so it shows a value of 0 for fully wet surface (evapotranspiration only limited by the atmospheric demand), and 1 for dry surfaces where there is no latent heat flux.

The WDI index could be expressed as follows,

$$WDI = 1 - \frac{ET_{act}}{ET_{pot}} = 1 - \left[\frac{(LST_{max} - T_a) - (LST - T_a)}{LST_{max} - T_a - (LST_{min} - T_a)} \right] \quad (8)$$

where LST_{max} and LST_{min} are maximum and minimum LST respectively; ET_{act} and ET_{pot} represent actual and potential evapotranspiration respectively, found for a given vegetation cover (or vegetation index) in the left and right edges of the trapezoid VITT (Vegetation index versus difference of temperature). Then, T_a represents air temperature. Verstraeten *et al.* (2001, in Ranjan, 2006) reformulated the WDI index equation,

based on the trapezoid, considering the difference of temperature on the ordinate axis and the vegetation index on the abscissa axis.

Other indexes

- **STI index**

The Standardized Thermal Index (STI) describes the deviation experienced LST with respect to the air temperature, as the drought conditions are accentuated (Park *et al.*, 2004). The STI index is based on the hypothesis that water-stressed areas present low values of NDVI and temperature gradients between the surface and the air, higher than in non-drought conditions. Therefore, the variation of this gradient will be inversely related to soil moisture and evapotranspiration of the area, and directly related to water stress.

The indicator ranges between 0 and 1, and it is defined by the following equation (Park *et al.*, 2004):

$$STI = \frac{(LST - T_{air_mean})_{acum}}{(LST + T_{air_mean})_{acum}} \quad (9)$$

where T_{air_mean} is the mean air temperature. The STI index values show a significant correlation with the deviation of the NDVI. This demonstrates that higher values of STI correspond with more severe droughts.

Several studies have shown that the cumulative deviations of LST present significant negative relationships with soil moisture content and the ratio ET_{act}/ET_{pot} , while they have positive relationships with the ration moisture deficit/ ET_{pot} . Then, it was found that STI values of 0.2 correspond to a decline of 15 % in NDVI, making this the threshold for thermal detection of drought conditions.

- **SIWSI index**

Physical models based on radiative transfer have shown that changes in water content of plant tissues present a large effect on leaf reflectance in several regions of the spectrum between the wavelengths of 0.4 to 2.5 μm . A major absorption value is presented in these wavelengths by foliar surfaces in well-hydrated tissues.

The reflectance is inversely related to water content (Ceccato *et al.*, 2001), therefore an increase in the value of reflectance at these wavelengths implies in most cases a plant response to some type of stress, including water stress (Carter, 1994). In this case, it is possible to obtain a direct measurement of water content in plants. The region of the spectrum in which these changes occur is the short-wave infrared range 1.3-2.5 μm (SIR, Short Infrared), where the amount of water available in the internal structure of the leaf controls the spectral reflectance (Tucker, 1980). To illustrate this fact, Fig. 4 represents the location of the bands 5 and 6 of MODIS sensor (TERRA satellite of NASA), and the reflectance of a vegetated surface with different soil moisture content (CW).

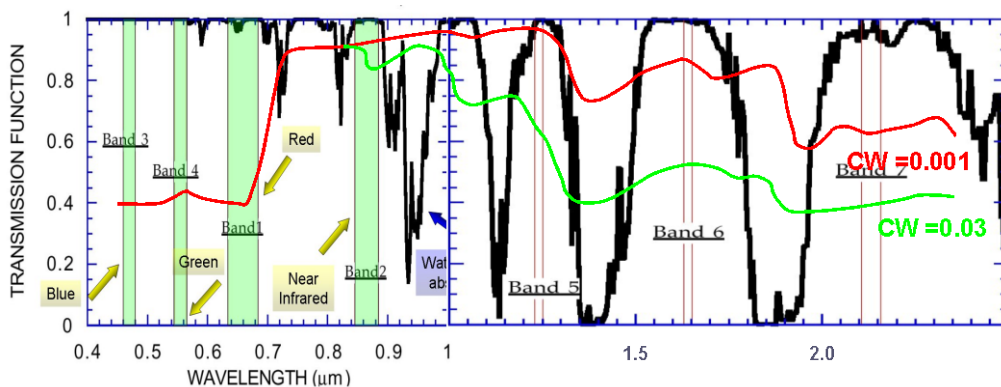


Fig. 4. Representation of MODIS sensor bands (source: Fensholt and Sandholt, 2003).

The reflectance of bare soil, leaf biochemical parameters, internal structure, leaf area index and the influence of the atmosphere affect the value of reflectance measured by satellite. Therefore, the influence of water in the tissues of the plant is needed for it to be independent of other factors. The SIWSI index with its formulation seeks to achieve this objective, and can be expressed considering the 6 band (eq. 8) or 5 band (eq. 9) of MODIS, which, as was seen from Figure 4, can discern these differences,

$$SIWSI(6,2) = (\rho_6 - \rho_2) / (\rho_6 + \rho_2) \quad (10)$$

$$SIWSI(5,2) = (\rho_5 - \rho_2) / (\rho_5 + \rho_2) \quad (11)$$

where ρ is the reflectance in the spectral range of MODIS 841 a 876 nm in the band 2, 1230 a 1250nm in the band 5 and 1628 to 1652 nm in the band 6. The SIWSI values from both equations are normalized, varying from -1 to 1. A positive value represents water stress on vegetation.

Classification of methodologies for estimation of ET_{act}

- Models based on surface energy balance

The energy balance equation, without advection, is expressed as:

$$R_N = \lambda ET + H + G + PH \quad (12)$$

where R_N is the net radiation, λET is the latent heat flux or ET_{act} (λ latent heat of vaporization and ET flux of evaporated water), H is the sensible heat flux, G is the soil heat flux, and PH the energy used in the photosynthesis process. The magnitude order of PH is generally small, it is therefore negligible. The residual equation is usually used for the estimation of λET considering the following equation (Choudhury, 1994),

$$\lambda ET = R_N - G - H \quad (13)$$

However, when ET-retrieval methods from remote sensing are used, several uncertainties arise in the parameterization of the energy term ($R_N - G$), and especially of the term G , which can reach high values in arid and semiarid countries (SIRRIMED D4.3, 2011).

- Models based on land surface temperature: derivations of the residual method

The surfaces where evapotranspiration occurs present a reduction in the temperature with respect to the non-evaporative surfaces. The level at which you set the surface temperature is an indicator of the distribution of the surface energy available for processes such as the flow of sensible and latent heat to the atmosphere, sensible heat flux to the ground and radiation into the atmosphere. The land surface temperature is a piece of readily-available remote sensing data. So, another expression derived from the residual equation, and known as "simplified equation", was derived for the assessment of ET_{act} (Jackson *et al.*, 1977; Delegido *et al.*, 1993),

$$ET_d = R_{Nd}^* - B \cdot (LST - T_a)_i \quad (14)$$

where ET_d is the daily actual evapotranspiration, R_{Nd}^* is the daily net radiation (mm/day), B is an empirical constant, and $(LST - T_a)_i$ is the difference between soil and air temperature, both measured around noon.

For the determination of the constant B , measures of: evapotranspiration (lysimeter, method of "eddy-correlation" method of Bowen), daily net radiation, daily mean air temperature and land surface temperature (which is obtained through remote sensing) are all needed. With these data, the constant B is calculated from

the regression line ($ET_d - R_{Nd}^*$) as a function of $(LST - T_a)_i$. Once B is obtained, it is possible to use the simplified equation for estimating evapotranspiration from LST , T_a and R_{Nd} data.

Later, this equation was improved by introducing a second parameter. A (Seguin, 1993):

$$ET_d = R_{Nd}^* + A - B \cdot (LST - T_a)_i \quad (15)$$

Net radiation data are difficult to obtain from conventional weather stations, which could therefore be a drawback for the simplified method. But, nowadays, estimation of net radiation could be obtained considering remote sensing data. However, the equation was modified to obtain an expression depending on global radiation (which is easier to get). The ET_0 is obtained with the following equation (Caselles *et al.*, 1992),

$$ET_0 = A \cdot T_a^{max} \cdot R_g + B \cdot R_g + C \quad (16)$$

where ET_0 is the reference crop evapotranspiration, T_a^{max} is the maximum air temperature, R_g daily global radiation, and A , B and C are empirical coefficients. There are several methods for estimating T_a^{max} and R_g from information obtained by remote sensing (Dedieu *et al.*, 1987).

- **Models based on the relationship between vegetation indexes and land surface temperature**

A negative linear relationship between land surface temperature and vegetation indices (such as NDVI Normalized Vegetation Index), is generally observed. The land surface temperature (LST) decreases as the density of vegetation increases, which is explained by the cooling caused by ET_{act} (Caselles *et al.*, 1998). The slope of this linear relationship varies depending on the soil water availability, which depends on water balance (rainfall and evaporation).

There are several water stress indices based on remote sensing of LST, associating the ET_{act} with potential ET (ET_{pot}) to assess water requirements.

One of the first that was developed is the **CWSI** (Crop Water Stress Index), expressed as (Jackson *et al.*, 1981),

$$\frac{ET_{act}}{ET_{pot}} = \frac{LST - LST_{max}}{LST_{min} - LST_{max}} = 1 - CWSI \quad (17)$$

where ET_{act} is the actual evapotranspiration, ET_{pot} is the potential evapotranspiration, LST_{max} is the maximum LST in the study area, and LST_{min} is the minimum LST in the study area (Jackson *et al.*, 1981). This index is reliable only for surfaces with full cover of vegetation.

For composite surfaces (only partially covered by vegetation), a graphical method of *VITT trapezoid* (Vegetation Index/Temperature Trapezoid), presented in Fig. 5, is used. With this method it is possible to estimate the *WDI index* (Water Deficit Index, Moran *et al.*, 1994).

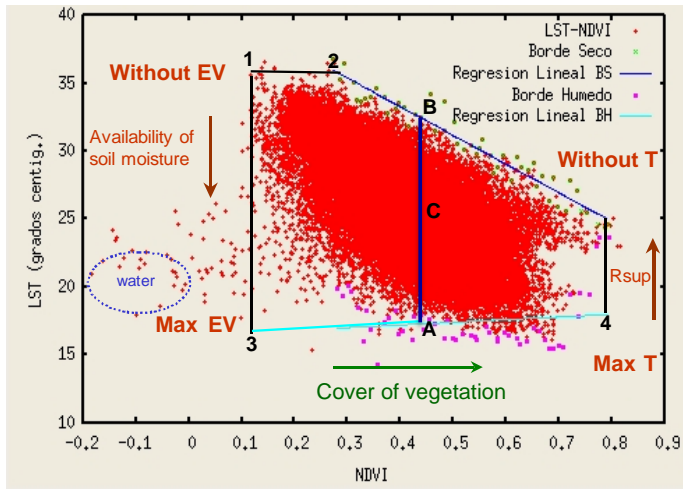


Fig. 5. VITT trapezoid (Vegetation Index-Temperature Trapezoid). Example for MODIS data, for Jucar River basin.

• Indirect methods. SVAT Model

These methods are based in Soil-Vegetation-Atmospheric Transfer (Soil-Vegetation-Atmosphere Transfer, SVAT) models. The SVAT models require data from different wavelengths (while the methods mentioned thus far require mainly data in the thermal infrared or IRR), to calculate land surface characteristics such as albedo, emissivity and leaf area index (LAI) (Courault *et al.*, 2003).

Although SVAT models are designed to be coupled with atmospheric models, they can also be used to study the processes of evapotranspiration in an "off-line" mode (Bastiaanssen *et al.*, 2005). These models are suitable for ET evaluation in precision irrigation for short periods of time (hours), but have the disadvantage of requiring more initial data.

Algorithms derived from the residual method

All the selected algorithms are derived from the *residual method*. Once all the terms of surface energy balance equation have been estimated, ET_{act} is evaluated as the residual of the equation. The methodologies considered could be classified into two groups:

- Methods with direct estimation of sensible heat flux (H_s), estimating ET as the residual term of the surface energy balance equation:
 - SM method (Simplified method),
 - SEBAL model (Surface Energy Balance Algorithm for Land), and
 - TSEB (Two Source Energy Balance model).

These are a direct application of the residual method, where:

$$\lambda ET = R_N - H_s - G \quad (18)$$

- Methods with direct estimation of evaporative fraction (EF), and therefore ET_{act} (without estimation of H_s):
 - Simplified SEBI method, S-SEBI (Soil Energy Balance Index), and
 - JIC method (proposed by Jiang and Islam, 2001).

Where:

$$\lambda ET = EF \cdot (R_N - G) \quad (19)$$

Three of these methods (S-SEBI, SEBAL and JIC) are based on the contrast between the pixels of the wet zone and the dry zone. These methods require a prior graphical representation and interpretation of the data, therefore they are also named *graphical methods*. The net radiation R_N , at daily scale, as well as the flux of soil heat G , are needed for ET_{act} estimation.

1. The Simplified Method

In the simplified method, proposed by Carlson *et al.* (1995), the net daily evapotranspiration integrated in the surface ET_d , is estimated from a few data: LST near noon, when the satellite passes ($T_{s,i}$), air temperature ($T_{a,i}$), and net radiation expressed as the integrated value over 24 hours ($R_{n,d}$), as follows

$$R_{n,d} - \lambda ET_d = B \cdot (T_{s,i} - T_{a,i})^n \quad (20)$$

where B and n are parameters to be defined. $R_{n,d}$ and λET are expressed in $cm \text{ día}^{-1}$. The term on the right of equation (9), represents an approximation of the daily sensible heat flux $H_{s,d}$, assuming that the soil heat flux is negligible at daily scale ($G_d \approx 0$). The term B could be considered as a coefficient of sensible heat flux transference by convection and n is a correction factor to take the stability of the atmosphere into account. An *unstable* situation (during the day, when the warmer air is below the cooler air), tends to increase the sensible heat flux, while the reverse situation (*stable* atmosphere), tends to inhibit this flux. Carlson *et al.* proposed a relationship among the B and n parameters, the vegetation fraction F_v and the corrected NDVI N^* , using the results from a SVAT simulation.

This method requires the following data:

- Spectral radiances in the red and NIR (for NDVI estimation), and LST, from remote sensing.
- Air temperature at surface level.

The main advantage of the simplified method is its simplicity. The drawback is its lack of precision, since the B and n parameters depend not only on the vegetation cover, but also of roughness height, wind velocity, and water status of soil and vegetation.

• The SEBAL method

The SEBAL method developed by Bastiaanssen *et al.* (1998) is a direct application of the residual method, combining an empirical and physical parameterization. The input data include local meteorological data (mainly wind velocity), and remote sensing data (radiances and LST). From these data, the net radiation (R_n), NDVI, albedo (α), roughness height (z_0) and soil heat flux (G), are estimated. The sensible heat flux is estimated by contrasting two sites (one site of wet soil or with vegetation without water stress, and another site of dry soil). ET_{act} is derived as the residual term of the surface energy balance.

• The TSEB algorithm

So far, the models presented consider a single source of water vapor at the surface. They do not distinguish contributions of vegetation and soil in the surface fluxes. Therefore, the use or the water stress of vegetation cannot be separated. In the models with the approach known as “Two sources” (Norman *et al.*, 1995; Kustas *et al.*, 2003; Melesse *et al.*, 2005), the estimation of surface energy balance at the surface is divided into two parts: one is related with the vegetation, and the other with the soil.

This model can reach, in certain cases, high accuracy (up to 90 %), but it is more complex than other approaches, and requires very accurate LST information.

• The S-SEBI algorithm

The S-SEBI scheme, proposed by Roerink et al. (2000), defines two temperature thresholds for a given surface albedo value: a maximum temperature, which corresponds to completely dry areas and a minimum temperature corresponding to surfaces that evaporate freely. These temperatures define the variation range of LST over the whole image, and are used for defining the evaporative fraction (EF). In the SEBI (Surface Energy Balance Index) method, the evapotranspiration estimated from the evaporative fraction is defined as follows,

$$EF = \frac{\lambda ET}{R_N - G} = \frac{\lambda ET}{\lambda ET + H_s} \quad (21)$$

The S-SEBI method presents two main advantages:

- It is a self-sufficient method while satellite data is available, and needs no ground measurement data.
- From a physical point of view, and comparing it with the methods that determine a single temperature for both dry and wet conditions, the S-SEBI method is more realistic because it determines the value of these temperatures as a function of albedo.

The data required for the application of this method are: spectral radiances in the visible, near infrared and thermal infrared.

• The JIC algorithm

The method proposed by Jiang et al. (2004), or the JIC method, is based on the analysis of LST-NDVI space. This space (triangular or trapezoidal form), delimited by the distribution of pixels, has a linear relationship with the surface fluxes of energy.

Fig. 6 below presents an example of LST-NDVI space obtained from remote sensing. This triangle defines the limits for the evaporative fraction (EF). The estimation of latent heat flux is restricted in this space, which is the key to this method. From this space, the EF is linearly related with LST for a certain NDVI.

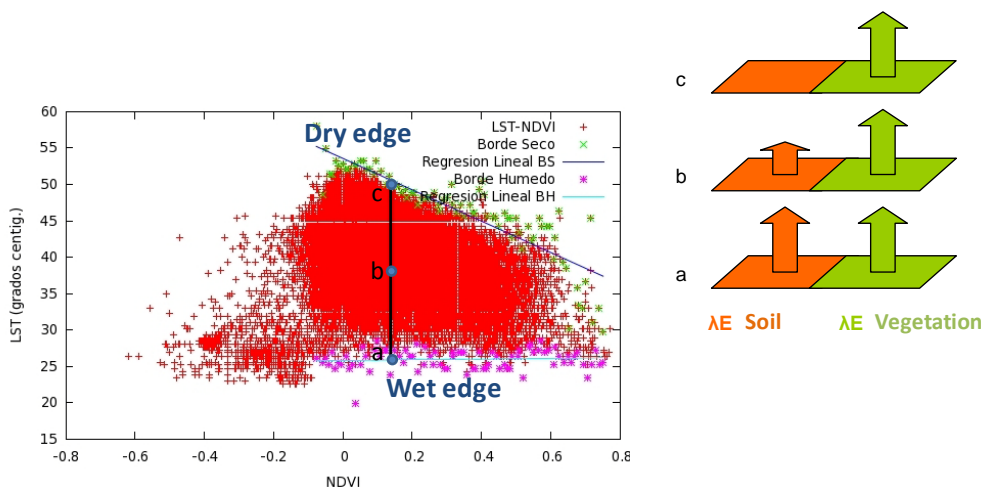


Fig. 6. Conceptual interpretation of LST vs. NDVI (adapted from Jiang et al., 2004). Example from MODIS data.

In this method, E_{Tact} is based in the *Priesler-Taylor* equation and a relation between LST and NDVI (Jiang and Islam, 2001), is estimated as follows:

$$\lambda ET = \phi \frac{\Delta}{(\Delta + \gamma)} (R_N - G) \quad (22)$$

where Φ is the evaporative fraction (EF), Δ is the slope of the vapor pressure, γ the psychometric constant and R_N represents net radiation.

In conditions without convection and advection,

$$ET \leq (R_N - G) \quad (23)$$

Therefore, Φ presents the following range corresponding to minimum and maximum values of ET_{act} , respectively.

$$0 \leq \phi \leq \frac{\Delta}{(\Delta + \gamma)} \quad (24)$$

Each pixel of this LST-NDVI space has an associated specific Φ defined by:

$$\phi = \phi_{max} \frac{LST_{max} - LST}{LST_{max} - LST_{min}} \quad (25)$$

where $\Phi_{max} = 1.26$ corresponds to bare soil, LST_{max} is the maximum LST for $NDVI=0$, and LST_{min} the minimum LST. Then, a spatial distribution of Φ is obtained for each date.

The following equation represents the evaporative fraction (EF),

$$EF = \phi \frac{\Delta}{(\Delta + \gamma)} \quad (26)$$

where the γ psychometric constant is a function of atmospheric pressure.

Application of Triangle method for estimation of ET_{act}

Datasets: Collection of spatio-temporal information

Several sources of information were considered, the National Plan of Remote Sensing (PNT), the CHS water agency, the Instituto Murciano de Investigación Agraria y Alimentaria (IMIDA), and information freely accessible by internet.

The satellite data used corresponded to Landsat 5 TM (TM5), Spot 5, and MODIS data. However, the work was mainly based on Landsat 5 TM and MODIS data. The MODIS (Moderate Resolution Imaging Spectroradiometer) is a sensor, on TERRA (EOS AM) and AQUA (EOS PM) platforms of NASA.

The Landsat images cover a total surface of 185x185 km². These images were geometrically rectified, and georeferenced considering the ETRS-89 system with UTM projection by the Instituto Geográfico Nacional (IGN).

For considering the whole SRB in a specified date, the acquisition of the following four images are needed: 199-33, 199-34, 200-33, and 200-34 (Fig. 7). A lag time between 199-33/1999-34 and 200-33/200-34 will be identified. Therefore, it is not possible to study the whole basin for the same date. The Region of Murcia is included in the spatial framework of 199-33 and 199-34 images.

For this study, the zones 199-33, 199-34, 200-33 and 200-34 were considered for years 2008 and 2009. Some of these images present a high percentage of cloudiness, especially in the case of 2008. For filtering clouds a methodology proposed by IGN was considered. This methodology of filtering is based in the difference between a reference image and the image to be evaluated (excluding the false positives, fixing a threshold in the thermal band).

Time series of meteorological information (air temperature, relative humidity, atmospheric water vapor, etc.), were collected for the same time period from IMIDA and National Agency of Meteorology (AEMET, Agencia Estatal de Meteorología). The IMIDA institute is the responsible for management of several meteorological and agrometeorological networks, with more than 100 gauging stations in the Region of Murcia (and more than 30 station of radiation measures). The following Fig. 8, represents the spatial distribution of stations for Region of Murcia.

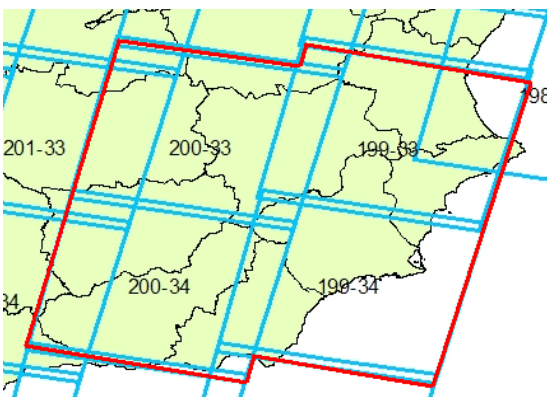


Fig. 7. Distribution of Landsat images over Spain.

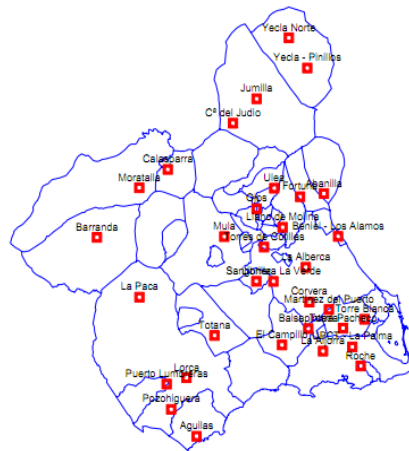


Fig. 8. Meteorological stations in the Murcia Region. Source: IMIDA on line.

The dataset was completed including products of MODIS images, provided by TERRA MODIS satellite (NASA), corresponding to the same date of TM5 images. The land surface temperature (LST) product presents a spatial resolution of 1 by 1 km. The acquisition of MODIS images is free, and these are available by internet (<http://ladsweb.nascom.nasa.gov/data/>).

Additional spatial information was collected and processed below GIS, in the present work, corresponding to channel network, UDAs, and administrative limits for SRB.

Estimation of time evolution of NDVI

Several vegetation indexes were considered, based in the interpretation of space conformed by LST and NDVI. Then, the water susceptibility (Giraut *et al.*, 2000) could be estimated based on one over of plant biomass based on NDVI (combination of bands 3 and 4); index of soil dryness (combination of bands 2 and 5), and cover of water surface (discrimination of band 7).

NDVI was derived from reflectance values in the Red (B3) and infrared (B4) region of electromagnetic spectrum of TM5 images, as follows:

$$NDVI = (B4 - B3) / (B4 + B3) \quad (27)$$

The range of NDVI correspond from -1 to 1, but for this study the range 0 (bare soil) to 1 (soil with maximum plant biomass), was considered. Then, negative values represent water. The Fig. 9 shows the spatial distribution of NDVI for two dates (14/02 and 24/07 of 2009), in the Region of Murcia.

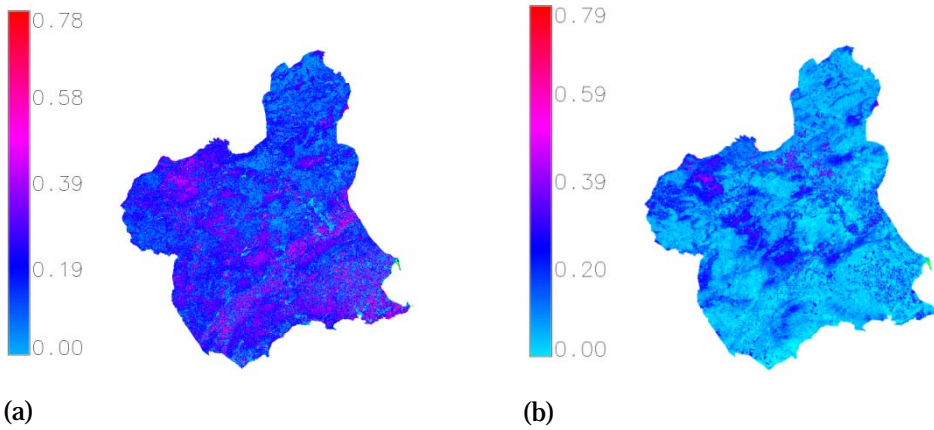


Fig. 9. Spatial distribution of NDVI for Murcia Region, from TM5: (a) 14/02/2009 and (b) 24/07/2009.

Estimation of time evolution of LST

From band 6 of Landsat, with spatial resolution of 120 m, the LST was estimated. The LST spatial distribution in combination with vegetation indexes will be considered in the estimation of indicators related with soil moisture (Sandholt *et al.*, 2002) and actual evapotranspiration (Jiang and Islam, 2001). The LST spatial distributions from TM5 were contrasted with the LST product provided by MODIS sensor. SPOT images have not present thermal band.

In the following paragraphs, the methodology for the estimation of LST from Landsat, is presented. The geometric correction was not needed for Landsat images, because correspond to PNT, and the corrections were done. The signals received by the thermal sensors (TM5) can be converted to at-sensor radiance (L_{sensor}), according the corrections proposed by Voogt and Oke (2003):

- (1) Spectral radiance conversion to at-sensor brightness temperature,
- (2) Correction by atmospheric absorption and re-emission,
- (3) Correction by surface emissivity, and
- (4) Correction by surface roughness.

In the case of correction (1), the signal received from thermal sensor could be converted to different parameters for the LST estimation,

$$L_{sensor} = gain.DN + bias \quad (28)$$

where L_{sensor} is the spectral radiance of thermal band, DN is the digital number of a given pixel (in this case, each pixel of TM5 band 6), $gain$ is the slope of the radiance/ DN conversion function depending of the band (for the band 6, the $gain$ is 0.055158), and $bias$ is the intercept of the radiance/ DN conversion function, it is a constant depending of the band ($bias=1.238$ for TM5 band 6)

$$T_{sensor} = \frac{K_2}{\ln\left(\frac{K_1}{L_{sensor}} + 1\right)} \quad (29)$$

where T_{sensor} represents the at-sensor brightness temperature (K) with $K_1=607.76$ W/(m²sr.μm) and $K_2=1260.56$ K as prelaunch calibration constants for TM5 (Landsat Project Science Office, 2002), and L_{sensor} estimated above.

For obtaining LST, the following steps corresponds to correction (2) to (4), applying the single-channel algorithm proposed by Jiménez-Muñoz and Sobrino (2003), must be done.

$$T_s = \gamma \left[\varepsilon^{-1} (\psi_1 L_{sensor} + \psi_2) + \psi_3 \right] + \delta \quad (30)$$

with

$$\gamma = \left\{ \frac{c^2 L_{sensor}}{T_{sensor}^2} \left[\frac{\lambda^4}{c_1} L_{sensor} + \lambda^{-1} \right] \right\}^{-1} \quad (31)$$

$$\delta = -\gamma L_{sensor} + T_{sensor} \quad (32)$$

where T_s is the LST in K, ε is the ground surface emissivity, $c_1=1.19104 \cdot 10^8$ ($W \mu m^4 m^{-2} sr^{-1}$), and $c^2=14387.7$ ($\mu m K$), λ is the effective wave length (μm) corresponding to band 6.

The following equations represent the correction by total atmospheric water vapor content (w in grs/cm^2), therefore the atmospheric functions (ψ_1 , ψ_2 and ψ_3) are depending only of w , particularized for TM/ETM+ 6 data, as follows,

$$\begin{aligned} \psi_1 &= 0.14714w^2 - 0.15583w + 1.1234 \\ \psi_2 &= -1.1836w^2 - 0.37607w - 0.52894 \\ \psi_3 &= -0.04554w^2 + 1.8719w - 0.39071 \end{aligned} \quad (33)$$

For the estimation of atmospheric water vapor, external data are needed. In this case, the MODIS Terra Level 2 Water Vapour product MOD05_L2 (Gao and Kaufman, 1998), could be used because the hour of satellite pass through the Iberian Peninsula is similar to Landsat. But the MODIS data are available from 2000, therefore for previous years the AVHRR sensor of NOAA satellite could be considered.

However, in the present work the maps of water vapor (grs/cm^2) were generated from monthly values provided for typical clear days by SoDA Project (<http://www.soda-is.com>) stations in different parts of the Region of Murcia, according to Remund *et al.* (2003).

The last step for the estimation of LST from Landsat, is the calculation of the surface emissivity (ε). The ε values could be obtained for example based on classification image, based on NDVI image or based on the ratio values of vegetation and bare ground (Zhang *et al.*, 2006). In this work, the ε values are estimated in function of NDVI (Valor and Caselles, 1996) as follows,

$$\begin{aligned} -1 < NDVI < -0.18 & \quad \varepsilon = 0.985 \\ -0.18 < NDVI < 0.157 & \quad \varepsilon = 0.955 \\ 0.157 < NDVI < 0.727 & \quad \varepsilon = 1.0094 + 0.047 \ln(NDVI) \\ 0.727 < NDVI < 1 & \quad \varepsilon = 0.99 \end{aligned} \quad (34)$$

The Fig. 10 presents an example of the application of the methodology described in the estimation of LST for Murcia Region (date 24/07/2009).

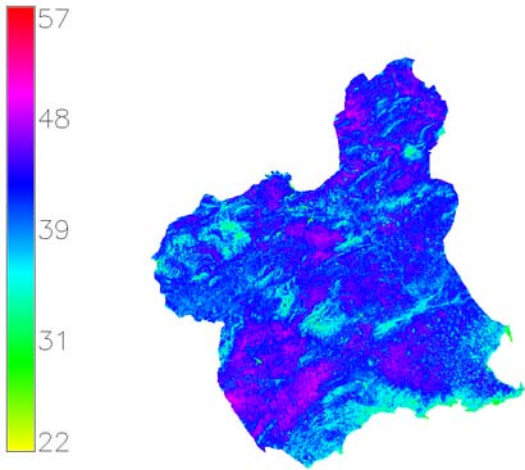


Fig. 10. Spatial distribution of LST (°C) for date 24/07/2009 (LSTD20090724).

The results of NDVI and LST derived from TM5, could be compared with the corresponding products from MODIS TERRA. In this case, the product MOD11A1 (daily LST with spatial resolution 1x1 km) and product MOD09GA (daily reflectances with spatial resolution 500x500 m), could be used. From MOD09GA the NDVI is estimated, combining the bands 1 and 2, as $NDVI = (B2-B1)/(B2+B1)$. From the comparison of images, the differences detected are negligible.

Application of JIC Algorithm derived from the residual method

An algorithm derived from *residual method*, proposed by Jiang *et al.* (2004) or JIC method, was selected. In the JIC method, the ET_{act} is based on the direct estimation of evaporative fraction (EF), without estimation of H_s , as follows

$$\lambda ET = \phi \frac{\Delta}{(\Delta + \gamma)} (R_N - G) \quad (35)$$

where ϕ is the evaporative fraction (EF), Δ is the slope of the vapour pressure, γ the psychrometric constant, R_N is the net radiation, and G is the the flux of soil heat.

This method require a prior graphical representation and interpretation of LST-NDVI space. This space (triangular or trapezoidal form), delimited by the distribution of pixels, has a linear relationship with the surface fluxes of energy. Each pixel of the space, presents an specific ϕ defined by,

$$\phi = \phi_{max} \frac{LST_{max} - LST}{LST_{max} - LST_{min}} \quad (36)$$

where $\phi_{max} = 1.26$ corresponds to bare soil, LST_{max} is the maximum LST for NDVI=0, and LST_{min} the minimum LST. Then, a spatial distribution of ϕ es obtained for each date.

The following equation represents the evaporative fraction (EF),

$$EF = \phi \frac{\Delta}{(\Delta + \gamma)} \quad (37)$$

where the γ psychrometric constant is function of atmospheric presion by the following equation,

$$\gamma = 0.665 \cdot 10^{-3} P \quad (38)$$

where P is the atmospheric pressure (kPa), depending of height (on normal climatology conditions), as :

$$P = P_0 e^{\left(\frac{-z}{8000}\right)} \quad (39)$$

where z is the height in meters above sea level, and P_0 atmospheric pressure (kPa) at sea level.

The Δ is the slope of the vapor pressure, is estimated as follows,

$$\Delta = \frac{4098 * 0.6108}{(T_a + 237.3)^2} \exp\left(\frac{17.27T_a}{T_a + 237.3}\right) \quad (40)$$

The maps of relative humidity (HR) and air temperature, are obtained from meteorological stations. The Fig. 11, presents an example of HR and T_a maps, for the date 24/07/2009. From these maps, the spatial distributions of e^* (saturated vapour pressure) and e_a (air vapour pressure), were derived.

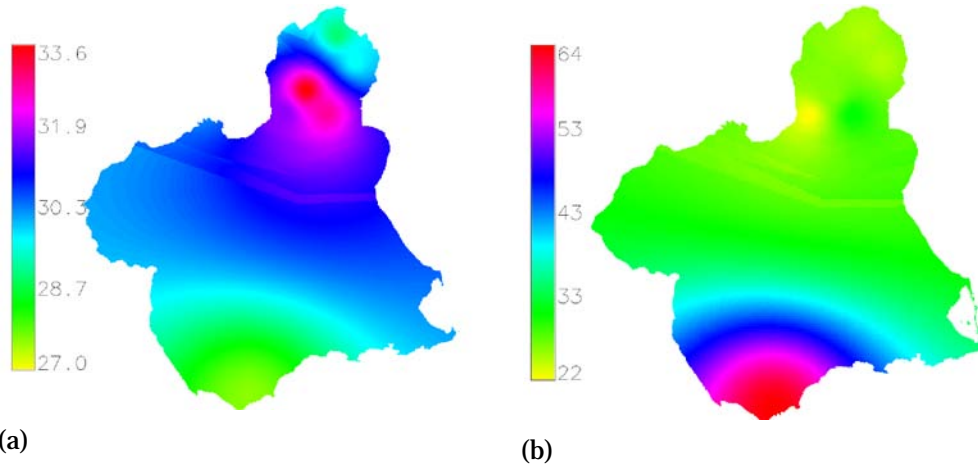


Fig. 11. Mean daily spatial distribution for Murcia Region: (a) T_a ($^{\circ}C$), and (b) HR .

The saturated vapour pressure (e^*) could be estimated, only depending of surface temperate. And, finally the e_a is estimated from HR (%) and e^* , as follows,

$$e_a = \frac{HR e^*}{100} \quad (41)$$

Estimation of net radiation

The net radiation ($R_N, Wm^{-2}day^{-1}$) is estimated considering ground meteorological data, remote sensing data, and topographical attributes derived from a Digital Elevation Model (DEM), applying the following equation,

$$R_N = R_s^{\downarrow} + R_s^{\uparrow} + R_L^{\downarrow} + R_L^{\uparrow} = (1 - \alpha)R_s^{\downarrow} + R_L^{\downarrow} + R_L^{\uparrow} \quad (42)$$

where R_s^\downarrow and R_s^\uparrow are downward and upward shortwave solar global radiation respectively, R_L^\downarrow and R_L^\uparrow are downward and upward long wave radiation respectively. They were estimated considering the Stefan Law, with the clear sky emissivity calculate from an empirical relationship with e_a , and the surface emissivity.

Estimation of $(R_s^\downarrow + R_s^\uparrow)$ shortwave net radiation

The diffuse, direct (beam) and ground reflected solar irradiation for given day, latitude, surface and atmospheric conditions, could be estimated for clear-sky and overcast atmospheric conditions with *r.sun* model below GRASS GIS (GRASS, 2011). Therefore, the term $(R_s^\downarrow + R_s^\uparrow)$ or net balance of shortwave global radiation, is derived from the results of *r.sun* command.

The *r.sun* model considers all relevant input parameters as spatially distributed entities to enable computations for large areas with complex terrain (Šúri and Hofierka, 2004). Conceptually the model is based on equaions of European Solar Radiation Atlas (ESRA). As an option the model considers a shadowing effect of the local topography. The *r.sun* works in two modes. In the first mode it calculates for the set local time a solar incidence angle (degrees) and solar irradiance values (Wm^{-2}). In the second mode, used in the present work, daily sums of solar radiation ($Whm^{-2}day^{-1}$) are computed within a set day.

The input data correspond to :

- A DEM (metres) and topographical attributes such as slope and aspect (both in decimal degrees), are used. In this case, a DEM with a spatial resolution of 30 m was considered. The topographical attributes were derived from the DEM, applying the GRASS GIS command *r.slope.aspect*. The following Fig. 12, presents the DEM and aspect maps for Murcia Region.

- *Latitude map* (decimal degrees, from -90° to 90°), is other map required.

Then, the spatial distribution of slope and latitude, are presented in Fig. 13.

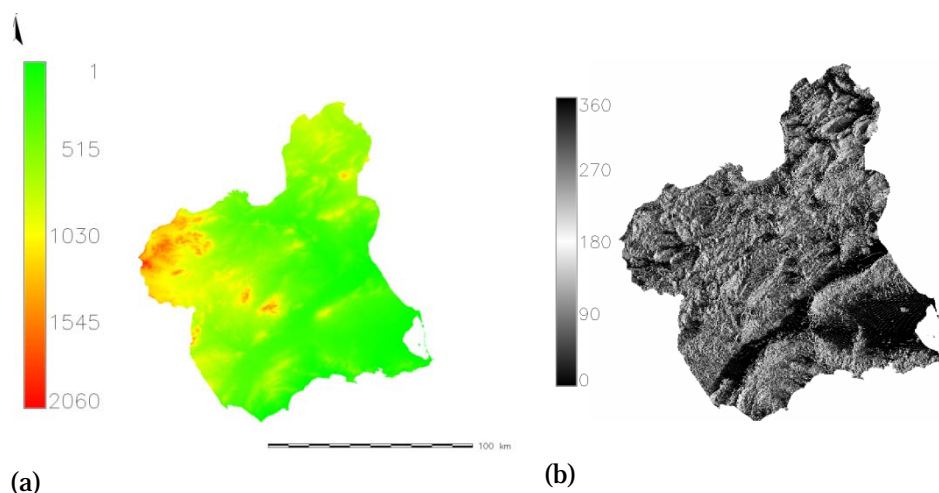


Fig. 12. Spatial distributions for Murcia Region: (a) DEM (m), and (b) aspect (grades from East).

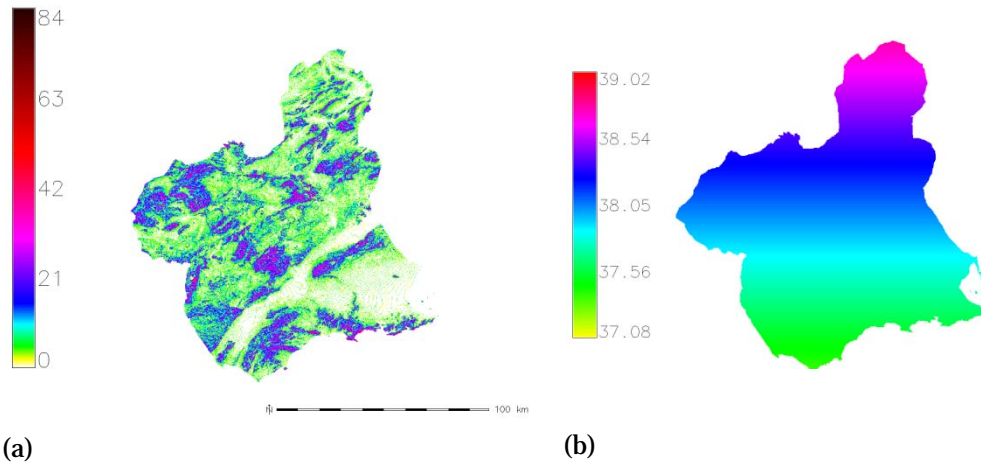


Fig. 13. Spatial distributions for Murcia Region: (a) slope, and (b) latitude.

- The *link turbidity* values, through SoDa Webpage (<http://www.helioclim.net>) were obtained at monthly scale for the 34 stations considered in the present study. The spatial distributions of monthly mean turbidity were obtained by interpolation
- The *albedo* indicates the percentage of irradiation reflected in function of the surface. In this case, the spatial distribution of albedo was derived from MODIS MOD43B3 product.
- The *day* corresponds to julian day of the year (1 to 365).

From the results of this command, the shortwave net radiation could be estimated from direct, diffuse and reflected radiation as follows,

$$R_N = R_{direct} - R_{diffuse} - R_{reflected} \quad (43)$$

Estimation of longwave net radiation

The longwave net radiation could be estimated by a balance between the radiation emitted by the sky and the reflected by earth's surface, as follows,

$$R_L^\downarrow - R_L^\uparrow = \sigma \varepsilon_a T_a^4 - \sigma \varepsilon_s LST^4 \quad (44)$$

where $\sigma = 5.67 \cdot 10^{-8} \text{Wm}^{-2}\text{K}^{-4}$, T_a (K), LST (K), and ε_a is the emissivity estimated as,

$$\varepsilon_a = \left[1 - (1 + \xi) \exp\left[-(1.2 + 3\xi)^{1/2}\right] \right] \text{ ó } \varepsilon_a = 0.56 + 0.259 \sqrt{e^0} \quad (45)$$

$$\xi = 46.5 \frac{e_a}{T_a} \quad (46)$$

where e_a air vapor pressure (kPa).

The heat flux from the soil G varying along the day, but its value is too small in comparison with R_N or λET . Therefore in the present work, the G value was not considered. . However, the relation among R_N , NDVI and G could be estimated by the Moran *et al.* (1989) equation,

$$G = 0.583 \exp\left[(-2.13NDVI)R_N\right] \approx 0 \quad (47)$$

Therefore, the actual evapotranspiration ($\text{Wm}^{-2}\text{day}^{-1}$) will be,

$$\lambda ET = \phi \frac{\Delta}{\Delta + \gamma} (R_N - G) \quad (48)$$

And for the result expressed in mm/day, is needed to divide eq. Xx by 3047.6 factor.

A schema of the developed methodology is presented in Fig. 14, and an example of spatial distributions of R_N and ET_{act} for the 24/07/09, are presented in Fig. 15.

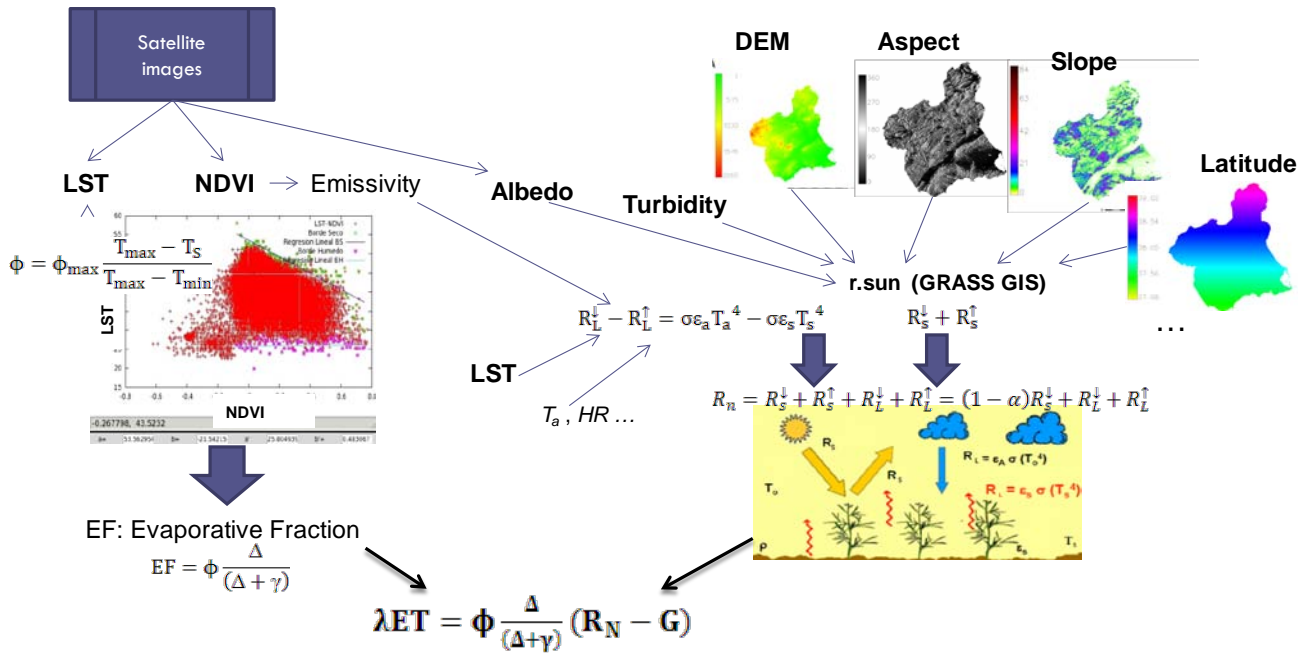


Fig. 14. Schema of the developed methodology.

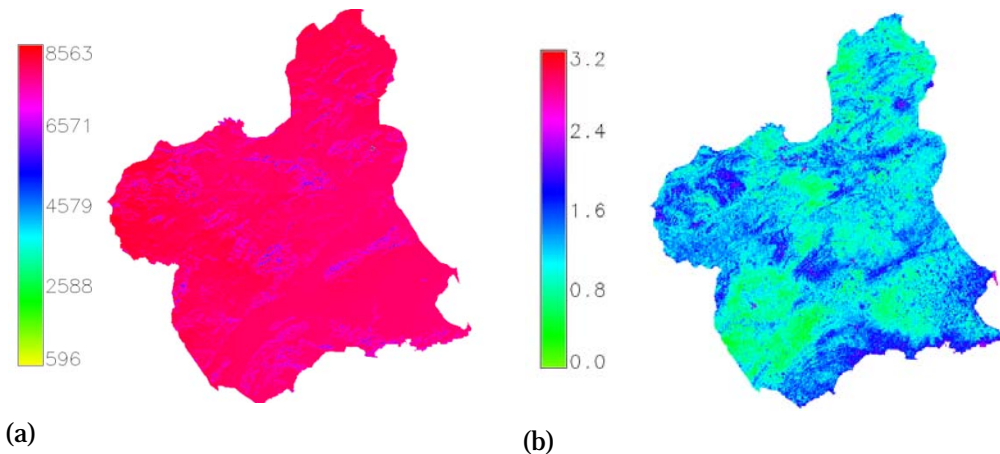


Fig. 15. Spatial distributions for Murcia Region: (a) R_N net radiation ($Wm^{-2}day^{-1}$), and (b) ET_{act} (mm/day).

References

- Andersen, J., Sandholt et al., I., Jensen, K.H., Refsgaard, J.C. y Gupta, H., 2002.** Perspectives in using a remotely sensed dryness index in distributed hydrological models at the river-basin scale. *Hydrological Processes*, 16, p. 2973-2987
- Baret, F. and Guyot, G., 1991.** Potentials and limits of vegetation indices for LAI and APAR assessment, *Remote Sensing of Environment*, 35, p. 161-173.
- Basso, B., Cammarano, D., De Vita, P., 2004.** Remotely sensed vegetation indices: theory and applications for crop management. *Rivista Italiana di Agrometeorologia*, (1), p. 36-53
- Bastiaanssen, W. G. M., Menenti, M., Feddes, R. A., Holtslag, A. A. M., 1998.** A remote sensing surface energy balance algorithm for land (SEBAL). 1. Formulation. *J. Hydrol.*, 212/213, p. 198-212.
- Bastiaanssen W.G.M., E. Noordman, J.M., Pelgrum, H., Davids, G., Thoreson, B.P., Allen, R.G., 2005.** SEBAL model with remotely sensed data to improve water-resources management under actual field conditions. *J. Irrig. Drainage Engin.*, 131, p. 85-93.
- Boegh, E., Soegaard, H., Hanan, N., Kabat, P. y Lesch, L., 1998.** A remote sensing study of the NDVI-Ts relationship and the transpiration from sparse vegetation in the Sahel based on high resolution satellite data. *Remote Sensing of Environment*, 69, p.224-240.
- Carlson, T.N. and Gillies, R.R., 1993.** A physical approach for inverting vegetation index with surface radiometric temperature to estimate surface soil water content.
- Carlson, T. N., Gillies, R. R., and Perry, E. M., 1994.** A method to make use of thermal infrared temperature and NDVI measurements to infer surface soil water content and fractional vegetation cover. *Remote Sensing Reviews*, 9, p. 161- 173.
- Carlson, T.N., William, J.C., Gillies, R.R., 1995.** A new look at the simplified method for remote sensing of daily evapotranspiration. *Remote Sens. Environ.*, 54, p. 161-167.
- Carlson T.N., 2007.** An Overview of the "Triangle Method" for Estimating Surface Evapotranspiration and Soil Moisture from Satellite Imagery. *Sensors*, 7, p. 1612-1629
- Caselles, V., Artigao, M., Hurtado, E., Coll, C., Brasa, A., 1998.** Mapping actual evapotranspiration by combining Landstat TM and NOAA-AVHRR images: application to the Barrax area, Albacete, Spain. *Remote Sensing of Environment*, 63, p. 1-10.
- Caselles, V., Delegido, G., Sobrino, J., Hurtado, E., 1992.** Evaluation of the maximum evapotranspiration over the La Mancha region, Spain, using NOAA AVHRR data. *International Journal of Remote Sensing*, 13 (5), p. 939-946.
- Carter, G. A., 1994.** Ratios of leaf reflectances in narrow wavebands as indicators of plant stress. *International Journal of Remote Sensing*, 15, p. 697- 703.
- Ceccato, P., Flasse, S., Tarantola, S., Jacquemoud, S., and Gregoire, J. M., 2001.** Detecting vegetation leaf water content using reflectance in the optical domain. *Remote Sensing of Environment*, 77, p. 22- 33.
- Czajkowski, K.P., 2000.** Thermal remote sensing of near-surface water vapor. *Remote Sensing of Environment*, 79 (1-2), p. 253-265.
- Choudhury, B., 1994.** Synergism of multispectral satellite observations for estimating regional land surface evaporation. *Remote Sensing of Environment*, 49, p. 264-274.
- Courault, D., Seguin, B., Olioso, A., 2003.** Review to estimate evapotranspiration from remote sensing data: some examples from the simplified relationship to the use of mesoscale atmospheric models. *ICID workshop on remote sensing of ET for large regions*, 17th September, 2003.
- Courault, D., Seguin, B., Olioso, A., 2005.** Review on estimation of evapotranspiration from remote sensing data: From empirical to numerical modeling approaches. *Irrigation and Drainage Systems*, 19, p. 223-249.
- Dedieu, G., Deschamps, P., Kerr, Y., 1987.** Satellite estimation of solar irradiance at the surface of the earth and of surface albedo using a physical model applied to METEOSAT data. *Journal of Climate and Applied Meteorology*, 26, p. 79-87.
- Delegido, J., Caselles, V., 1993.** Evapotranspiración. Teledetección en el seguimiento de los fenómenos naturales. *Climatología y Desertificación* (coordinadores de la edición S. Gandía y J. Meliá), Universidad de Valencia, p. 205-213.
- ESA, 2009.** ESA's Water Mission SMOS BR-278. European SA, BR-278, May 2009.

- Fensholt, R. y Sandholt, I., 2003.** Derivation of a shortwave infrared water stress index from MODIS near- and shortwave infrared data in a semiarid environment. *Remote Sensing of Environment*, 87 (1), p. 111-121.
- Gao, B.-C., and Kaufman, Y. J., 1998.** *The MODIS Near-IR Water Vapor Algorithm. Algorithm Technical Background Document. Product ID: MOD05 - Total Precipitable Water.* p. 1-23. On line http://modis-atmos.gsfc.nasa.gov/docs/atbd_mod03.pdf
- García Galiano, S.G., González Real, M.M., Baille, A., Martínez Álvarez, V., 2006.** Desarrollo de un sistema de alerta temprana frente a sequías a nivel regional para las cuencas del Río Júcar y Río Segura. Informe Final. Dirección General del Agua, Ministerio de Medio Ambiente.
- García Galiano, S.G., Giraldo Osorio, J.D., Urrea Mallebrera, M., Mérida Abril, A., Tetay Botía, C., 2011.** Assessing drought hazard under non-stationary conditions on South East of Spain. In: *Risk in Water Resources Management*. (Eds. G. Blöschl, K. Takeuchi, S. Jain, A. Farnleitner, A. Schumann). IAHS Publ. 347, IAHS Press, CEH Wallingford, Oxfordshire, United Kingdom, p. 85-91.
- Giraut, M., Minotti, P., Ludueña, S., 2000.** Integración de imágenes SAC-C, LANDSAT, y SPOT pancromático para la determinación de susceptibilidad hídrica. *IX Simposio Latinoamericano de Percepción Remota*, p. 1-8 (On line http://www.hidricosargentina.gov.ar/selper_bol_giraut.pdf)
- Gitelson, A., Kaufman, Y., Merzylak, M. 1996.** Use of a green channel in remote sensing of global vegetation from EOS-MODIS. *Remote Sensing of Environment*, 58: 289-298.
- Goetz, S. J., 1997.** Multisensor analysis of NDVI, surface temperature and biophysical variables at a mixed grassland site. *International Journal of Remote Sensing*, 18, p. 71-94.
- Goward, S.N., Xue, Y., y Czajkowski, K.P., 2002.** Evaluating land surface moisture conditions from the remotely sensed temperature/vegetation index measurements: An exploration with the simplified simple biosphere model. *Remote Sensing of Environment*, 79, p. 225-242.
- GRASS, 2011.** *GRASS (Geographic Resources Analysis Support System) GIS 6.4.2svn Reference Manual.* On line http://grass.osgeo.org/grass64/manuals/html64_user/index.html
- Huete, A., 1988.** A soil adjusted vegetation index (SAVI). *International Journal of Remote Sensing*, 9, p. 295-309.
- Jackson, R., Reginato, R., Idso, S.B., 1977.** Wheat canopy temperature: a practical tool for evaluating water requirements. *Water Resources Research*, 13, p. 651-656.
- Jackson, R., Idso, S., Reginato, R., Pinter, P., 1981.** Canopy temperature as a crop water stress indicator. *Water Resources Research*, 17, p. 1133-1138.
- Jiang, L., Islam, S. 2001.** Estimation of surface evaporation map over southern GreatPlains using remote sensing data. *Water Resources Research*, 37(2), p. 329-340.
- Jiang, L., Islam, S., Carlson, T.N., 2004.** Uncertainties in latent heat flux measurements and estimation: implications for using a simplified approach with remote sensing data. *Can. J. Remote Sensing*, 30, p. 769-787.
- Jiménez-Muñoz, J.C., Sobrino, J.A., 2003.** A generalized single-channel method for retrieving land surface temperature from remote sensing data. *Journal of Geophysical Research*, 108, 1.
- Jordan, C.F. 1969.** Derivation of leaf area index from quality measurements of light on the forest floor. *Ecology*, vol. 50, pp. 663-666.
- Kriegler, F. J., Malila, W. A., Nalepka, R. F., Richardson, W. 1969.** Preprocessing transformations and their effects on multispectral recognition, in: *Proceedings of the Sixth International Symposium on Remote Sensing of Environment*, University of Michigan, Ann Arbor, MI, p. 97-131
- Kustas, W.P., Norman, J.M., Anderson, M.C., French, A.N. (2003).** Estimating subpixel surface temperatures and energy fluxes from the vegetation index radiometric temperature relationship. *Remote Sens. Environ.*, 85, p. 429-440.
- Landsat Project Science Office, 2002.** Landsat 7 Science Data User's Handbook. Goddard Space Flight Center, Greenbelt, M.D.
- Moran M.S., Clarke T.R., Inoue Y., Vidal A., 1994.** Estimating crop water deficit using the relation between surface-air temperature and spectral vegetation index. *Remote Sens. Environ.*, 49, p. 246-263.
- Melesse, A.M., Nangia, V., 2005.** Estimation of spatially distributed surface energy fluxes using remotely-sensed data for agricultural fields. *Hydrological Processes*, 19, p. 2653-2670.

- Nemani, R.R and Running, S.W., 1989.** Estimation of regional surface resistance to evapotranspiration from NDVI and thermal IR AVHRR data. *Journal of Applied Meteorology*, 28, p. 276–284.
- Nemani, R., Pierce, L., Running, S. y Goward, S., 1993.** Developing satellite-derived estimates of surface moisture status. *Journal of Applied Meteorology*, 32 (3), p. 548–557.
- Norman, J.M., Kustas, W.P., Hume, K.S., 1995.** Source approach for estimating soil and vegetation energy fluxes in observations of directional radiometric surface temperature. *Agricultural and Forest Meteorology*, 27, p. 263-293.
- Olioso, A., Inoue, Y., Ortega-Farias, S., Demarty, J., Wigneron, J.-P., Braud, I., Jacob, F., Lecharpentier, P., Ottlé, C., Calvet, J.-C., Brisson, N., 2005.** Future directions for advanced evapotranspiration modeling: assimilation of remote sensing data into crop simulation models and SVAT models. *Irrigation and Drainage Systems*, 19, p. 377-412.
- Park, S., Feddema, J.J., and Egbert, S. L., 2004.** Impacts of hydrologic soil properties on drought detection with MODIS thermal data. *Remote Sensing of Environment*, 89, p. 53-62.
- Price, J. C., 1990.** Using spatial context in satellite data to infer regional scale evapotranspiration. *IEEE Transactions on Geoscience and Remote Sensing*, 28, p. 940–948.
- Prihodko, L. and Goward, S.N., 1997.** Estimation of air temperature from remotely sensed surface observations. *Remote Sensing of Environment*, 60 (3), p. 335–346.
- Richardson, A. J. and Everitt, J. H., 1992.** Using spectra vegetation indices to estimate rangeland productivity, *Geocarto International*, 1, p 63-69.
- Remund J., Wald L., Lefevre M., Ranchin T., Page J., 2003.** Worldwide Linke turbidity information. Proceedings of ISES Solar World Congress, 16-19 June 2003, Göteborg, Sweden). CD-ROM published by International Solar Energy Society. On line http://hal.archives-ouvertes.fr/docs/00/46/57/91/PDF/ises2003_linke.pdf
- Roerink, G.L., Su, Z., Meneti, N., 2000.** S-SEBI: A simple remote sensing algorithm to estimate the surface energy balance. *Phys. Chem. Earth (B)*, 25, p. 147-157.
- Rouse, J.W., R.H.Haas, J.A.Schell, and D.W.Deering, 1973.** Monitoring vegetation systems in the great plains with ERTS, *Third ERTS Symposium*, NASA SP-351 I, p. 309-317.
- Sandholt, I., Rasmussen, K. and Andersen, J., 2002.** A simple interpretation of the surface temperature/vegetation index space for assessment of surface moisture status. *Remote Sensing of Environment*, 79 (2-3), p. 213-224.
- Seguin, B., 1993.** NOAA/AVHRR data for crop monitoring at a regional level: possibilities and limits in the European context. *EARSeI Advances in Remote Sensing*, 2 (2), p. 87-93.
- SIRRIMED D4.3, 2011.** Deliverable D4.3. ET-retrieval algorithms for ET-Mapping: State-of-the-Art and Tools to be used in SIRRIMED WP4 and WP5. SIRRIMED Sustainable use of irrigation water in the Mediterranean Region. FP7 Seventh Framework Programme.
- SRBDAP. 2007.** *Segura River Basin Drought Action Plan*. Hydrographic Confederation of Segura River Basin (CHS), Ministry of Environment, Marine and Rural Affairs, Spain.
- Šúri, M., Hofierka, J. 2004.** A new GIS-based solar radiation model and its application to photovoltaic assessments. *Transactions in GIS*, 8(2), p. 175-190.
- Troufleau, D. y Soegaard, H., 1998.** Deriving surface water status in the Sahel from the Pathfinder AVHRR Land data set. *Physics and Chemistry of the Earth*, 23 (4), p. 421–426.
- Tucker, C. J., 1980.** Remote sensing of leaf water content in the near infrared. *Remote Sensing of Environment*, 10, p. 23– 32.
- Urrea Mallebrera, M., Mérida Abril, A., García Galiano, S.G., 2011.** Segura River Basin: Spanish Pilot River Basin Regarding Water Scarcity and Droughts. In: *Agricultural Drought Indices. Proceedings of the WMO/UNISDR Expert Group Meeting on Agricultural Drought Indices*. S. Mannava V.K., R.P. Motha, D.A. Wilhite and D.A. Wood (Eds.), 2-4 June 2010, Murcia, Spain: Geneva, Switzerland: World Meteorological Organization. AGM-11, WMO/TD No. 1572; WAOB-2011. 219 p. 2-12.
- Valor, E., Caselles, V., 1996.** Mapping land surface emissivity from NDVI: Application to European, African, and South American Areas. *Remote Sensing of Environment*, 57 (3), p. 167-184
- Voogt, J.A., Oke T.R., 2003.** Thermal remote sensing of urban climates. *Remote Sensing of Environment*, 86 (3),p. 370-384.

- Verstraeten, W.W., Veroustraete, F., and Feyen, J., 2001.** Monitoring water limited carbon mass fluxes over Europe using NOAA-AVHRR imagery and an adapted PEM Model C-FIX.
- Verstraeten, W.W., Veroustraete, F., Feyen, J., 2008.** Assessment of Evapotranspiration and Soil Moisture Content Across Different Scales of Observation. *Sensors*, 8, p. 70-117
- Wang, C., Qi, S., Niu, Z., and Wang, 2004.** Evaluating soil moisture status in China using the temperature-vegetation dryness index (TVDI). *Canadian Journal of Remote Sensing*, 30(5), p. 671-679.
- Zhang, J., Wang, Y., Li, Y., 2006.** A C++ program for retrieving land surface temperature from the data of Landsat TM/ETM+ band 6. *Computers & Geosciences*, 32, p. 1796-1805.